ISSN: 2579-5821 (Print)
ISSN: 2579-5546 (Online)
URL address: http://journal.unhas.ac.id/index.php/geocelebes
DOI: 10.70561/geocelebes.v10i1.49626

Jurnal Geocelebes Vol. 10 No. 1, April 2026, 82 – 95

Surface Ocean Current Variability Near Selayar Island During the Three El Niño-Southern Oscillation (ENSO) Phases

Andika*, Gladiva Warouw

Geophysics Department, Hasanuddin University, Makassar 90245, Indonesia.

*Corresponding author. Email: andika@unhas.ac.id

Manuscript received: 27 January 2026; Received in revised form: 25 March 2026; Accepted: 1 April 2026

Abstract

This study investigates the seasonal and interannual variability of surface ocean currents around Selayar Island, Indonesia, with a focus on differences among the three phases of the El Niño–Southern Oscillation (ENSO). Monthly surface current data from 1993 to 2020 were analyzed using climatological, composite, and anomaly approaches. The results reveal a spatially heterogeneous current structure that is dominated by seasonal variability, with domain-averaged current magnitudes ranging from approximately 0.085–0.305 ms^{-1}. Interannual variability related to ENSO is evident mainly in the magnitude of surface current anomalies, which range approximately 0.03–0.05 ms^{-1} during El Niño and increase to about 0.07–0.09 ms^{-1} during La Niña, with peak values reaching ~0.10–0.12 ms^{-1}. This indicates that ENSO primarily modulates current intensity rather than flow direction. Differences in anomaly direction are more pronounced under Neutral conditions, where anomaly patterns differ from those observed during both El Niño and La Niña phases. Overall, the results indicate that ENSO acts as an interannual modulation of surface currents, while monsoonal forcing remains the primary control on surface current dynamics in the study region.

Keywords: Anomaly; ENSO; Selayar; Surface Current; Variability,

Citation: Andika, A., & Warouw, G. (2026). Surface Ocean Current Variability Near Selayar Island During the Three El Niño-Southern Oscillation (ENSO) Phases. *Jurnal Geocelebes*, 10(1): 82–95, doi: 10.70561/geocelebes.v10i1.49626

Introduction

Sea surface currents are a key component of ocean dynamics, governing the redistribution of temperature (Gao et al., 2022; Elzahaby et al., 2021; Vijith et al., 2020), salinity (Laurindo et al., 2024; Ralston et al., 2024; Nie et al., 2023), sediments (Fu et al., 2024; Devis-Morales et al., 2021), plankton (Manral et al., 2023; Hu et al., 2021), nutrients (Li et al., 2022; Lu et al., 2020), and pollutants (Bhattacharya et al., 2026; Lefebvre et al., 2023) on daily to interannual timescales, while simultaneously defining major transport pathways for a wide range of oceanographic processes and human activities at sea. Owing to this cross-sectoral role, accurate knowledge of surface currents is increasingly recognized as a fundamental scientific and operational prerequisite for understanding ocean variability and for supporting safe and efficient maritime activities (Röhrs et al., 2021; Isern-Fontanet et al., 2017). In operational contexts, surface currents constitute a core input for drift predictions, including the tracking of drifting persons or objects (Trinanes et al., 2016), oil spill trajectory assessments (Bhattacharya et al., 2026; Keramea et al., 2021), modeling of marine debris and waste dispersion (Purba et al., 2024; Chassignet et al., 2021), and ship routing and navigation planning (Mannarini et al., 2024). In such applications, even small errors in surface current estimates can rapidly amplify into large trajectory deviations over timescales of hours to days (Röhrs et al., 2021).

The urgency of surface current research has increased in parallel with the growing demand for real-time ocean services and the rising exposure to risk in coastal and archipelagic regions. Studies in operational oceanography demonstrate that reliable surface current predictions contribute directly to the efficiency of search and rescue operations (Wang et al., 2025; Tamtare et al., 2022; Córdova & Flores, 2022; Mateus et al., 2020), the mitigation of maritime accidents (Zhu et al., 2023), and the reduction of pollution impacts (Bosi et al., 2021; Keramea et al., 2021), particularly when surface currents interact with winds and waves within the upper ocean layer (Röhrs et al., 2021).

The need for regional-scale studies is particularly pronounced in the Indonesian Archipelago, where monsoonal circulation, equatorial wave dynamics, and complex shallow deep ocean topography strongly interact (Yoneyama & Zhang, 2020; Xue et al., 2020). One of the most critical elements of this system is the Indonesian Throughflow (ITF), a large-scale transport of water masses from the Pacific to the Indian Ocean through the Indonesian seas, which plays a key role in inter-basin heat and freshwater exchange and exerts a significant influence on Indo-Pacific oceanography and climate (Feng et al., 2018). The ITF exhibits variability across seasonal to interannual timescales and is modulated by changes in monsoonal winds as well as large-scale climate modes such as the El Niño–Southern Oscillation (ENSO) and the Indian Ocean Dipole (IOD) (Zhu & Wang, 2024; Santoso et al., 2022; Feng et al., 2018). Along the primary ITF inflow pathway in the Makassar Strait, long-term observational records reveal pronounced intraseasonal, seasonal (monsoonal), and interannual fluctuations; at interannual timescales, the southward transport tends to weaken during El Niño events and strengthen during La Niña conditions (Gordon et al., 2019). This ITF–ENSO/IOD linkage underscores the potential for ENSO phase transitions to modify surface current dynamics in ITF corridors and branching regions, including the waters surrounding Selayar Island.

From an oceanographic perspective, the Selayar Slope in the southern Makassar Strait represents a confluence region where the ITF from the Makassar Strait meets the seasonally varying current system between the Java Sea and the Flores Sea, with additional influences from other regional dynamics. This setting gives rise to distinctive stratification structures and water mass characteristics (Prihatiningsih et al., 2021). Modeling evidence further indicates substantial water mass exchange within the triangle formed by the Java Sea, Makassar Strait, and Flores Sea, underscoring the strong monsoonal control and interbasin connectivity that shape regional circulation patterns (Apriansyah et al., 2024). At a more local scale, studies around the Selayar Islands have documented surface current patterns that vary in response to the monsoonal cycle and transitional seasons (Bayhaqi et al., 2017). Consequently, the waters surrounding Selayar are simultaneously influenced by monsoonal variability, ITF dynamics, and interannual climate variability, rendering surface current characteristics particularly sensitive to changes in regional ocean and atmosphere conditions.

Beyond its scientific relevance, Selayar Island and the surrounding waters are also of considerable importance for maritime safety. Ferry routes and maritime activities in this region have experienced several major accidents, including the sinking and grounding of the KMP/KM *Lestari Maju* in Selayar waters on 3 July 2018, which was widely reported by the media and authorities (Mappong, 2018), the sinking of two fishing vessels in February 2023 (Wardiyah, 2024), and the sinking of the cargo vessel KLM *Tahta Mandiri* on 10 August 2024 (Said, 2024). In this sense,

surface current research in the Selayar region carries an additional level of urgency, as it not only advances the understanding of physical oceanographic processes but also strengthens the information base for maritime safety services.

Nevertheless, existing studies in the Selayar region and its surroundings have predominantly focused on seasonal variability, stratification, and water mass connectivity (Bayhaqi et al., 2017; Prihatiningsih et al., 2021; Apriansyah et al., 2024), while a quantitative assessment of surface current responses to ENSO phases around Selayar, including changes in flow direction, current strengthening or weakening, and modifications of spatial current structure, remains relatively limited. This gap persists despite clear evidence of ENSO signals in current and transport variability within the Makassar Strait from long-term observations (Gordon et al., 2019), as well as climate modeling studies that demonstrate robust linkages between the ITF and both ENSO and the Indian Ocean Dipole (IOD) (Santoso et al., 2022). Accordingly, this study aims to quantify differences in surface ocean currents among ENSO phases (El Niño, La Niña, and Neutral) using composite and anomaly analyses of surface current speed and direction.

Data and Methods

Data

This study utilizes monthly sea surface current data obtained from the Copernicus Marine Environment Monitoring Service (CMEMS) Global Ocean Physics Reanalysis (https://doi.org/10.48670/moi-00021), produced by Mercator Ocean International (2026). The dataset consists of monthly mean fields with a horizontal resolution of 0.083° × 0.083° (approximately 1/12°), derived from the GLORYS12V1 reanalysis system based on the NEMO ocean model with assimilation of satellite observations and in-situ measurements (Jean-Michel et al., 2021). The analyzed variables include the eastward sea water velocity (u) and the northward sea water velocity (v) for the period January 1993 to December 2020. Vertically, surface currents are defined in this study as the simple average of the uppermost five model layers, spanning depths from 0.49 m to 5.08 m below the sea surface. This depth range is considered representative of near-surface ocean current dynamics. The study area is confined to waters surrounding Selayar Island and the southern Makassar Strait, covering a spatial extent of 6.92°S–5.33°S and 119.17°E–120.92°E (Figure 1). This domain is represented by a grid of 20 latitude points × 22 longitude points, which is sufficient to resolve mesoscale spatial variability of surface currents in the region.

To examine the influence of interannual climate variability, particularly ENSO, the monthly Niño-3.4 index (https://psl.noaa.gov/data/timeseries/month/DS/Nino34_CPC/) was employed and obtained from the NOAA Physical Sciences Laboratory (NOAA, 2026). The Niño-3.4 index is defined as the sea surface temperature anomaly (SSTA) averaged over the region 5°N–5°S and 170°–120°W, and is widely used as an indicator of ENSO phase and intensity (Wei, 2024; L'Heureux et al., 2024).

Methods

ENSO Phase Classification

Interannual variability is represented by the ENSO, which is classified using the monthly Niño-3.4 index. Each month during the analysis period (January 1993–December 2020) is categorized as El Niño when the Niño-3.4 SSTA is ≥ +0.5 °C, La Niña when it is ≤ −0.5 °C, and Neutral when it falls between these two thresholds (L'Heureux et al., 2024; Halide et al., 2024). Based on these criteria, a total of 336 months is classified into Neutral (N = 156), El Niño (N = 76), and La Niña (N = 104),

which are subsequently used in the composite analyses.

Surface Current Processing

In this study, surface currents are represented as a simple vertical average of the uppermost five model layers (0.49, 1.54, 2.65, 3.82, and 5.08 m) at each grid point and time step. This approach is used to characterize current dynamics within the near-surface ocean layer that is most relevant to surface oceanographic processes.

Surface currents are represented as two-dimensional vectors, and their magnitude is calculated using standard vector formulations (Stewart, 2008; Emery & Thomson, 2001). The climatological mean and anomalies are computed following standard statistical approaches (Wilks, 2011; Hartmann, 2016), while composite analysis is applied to extract ENSO-related variability (Boschat et al., 2016; Li & Dolman, 2023).

The notation (x, y, t) is used to denote the spatial and temporal dependence of the variables, where x and y represent longitude and latitude coordinates, respectively, and t denotes the monthly time index. The zonal and meridional components of the surface current velocity are expressed as $u(x, y, t)$ and $v(x, y, t)$, respectively.

Surface currents are represented as two-dimensional vectors, as shown in Equation (1):

$$\vec{U}(x, y, t) = \big(u(x, y, t), v(x, y, t)\big) \qquad (1)$$

The current speed (current magnitude) is calculated using the Equation (2):

$$\left|\vec{U}(x, y, t)\right| = \sqrt{u(x, y, t)^2 + v(x, y, t)^2} \qquad (2)$$

This magnitude is used to describe the intensity of the surface current, while current direction is assessed qualitatively based on the orientation of the current vectors.

Composite Analysis of Surface Currents

Composite analysis is employed to identify the mean surface current patterns associated with each ENSO phase. Composite methods are widely used in the geosciences to extract the typical characteristics of a given condition by averaging events that belong to a specific category (Li & Dolman, 2023; Boschat et al., 2016).

After the monthly data are grouped into El Niño, La Niña, and Neutral phases, surface current composites are calculated by averaging the zonal and meridional current components for each phase. For a given ENSO phase c with a total of N_c months, the composite current components are given by Equation (3) and (4):

$$u_c(x, y) = \frac{1}{N_c} \sum_{t \in c} u(x, y, t) \qquad (3)$$

$$v_c(x, y) = \frac{1}{N_c} \sum_{t \in c} v(x, y, t) \qquad (4)$$

The composite current magnitude is then calculated from the composite current components using the same formulation as for the individual data. This analysis is intended to highlight interannual variability signals associated with ENSO while suppressing short-term, random fluctuations.

Composite Analysis of Surface Currents Anomalies

Surface current anomaly analysis is conducted to examine deviations of the currents from their mean state. The mean zonal and meridional current components are calculated as time averages at each grid point over the entire analysis period and are denoted as $\bar{u}(x, y)$ and $\bar{v}(x, y)$, respectively.

The anomalies of the current components are given by Equation (5) and (6):

$$u'(x, y, t) = u(x, y, t) - \bar{u}(x, y) \qquad (5)$$

$$v'(x, y, t) = v(x, y, t) - \bar{v}(x, y) \qquad (6)$$

This approach computes anomalies as the difference between the raw current values and their corresponding mean values, calculated separately for the zonal and meridional components. The magnitude of the surface current anomaly vector is then calculated using the Equation (7):

$$\left|\vec{U}'(x,y,t)\right| = \sqrt{u'(x,y,t)^2 + v'(x,y,t)^2} \quad (7)$$

Composite anomalies for each ENSO phase are obtained by averaging the anomaly component values over all months belonging to the respective phase. This approach allows spatial patterns of surface current intensification or weakening relative to the long-term mean state to be consistently analyzed within a vector framework.

It should be noted that the magnitude of the surface current anomaly vector is always non-negative. This is a direct consequence of defining vector magnitude as the square root of the sum of squared zonal and meridional anomaly components. Although the anomaly components $u'$and v'may take either positive or negative values, the vector magnitude represents only the absolute strength of the deviation from the mean state and does not convey information on sign or direction. Accordingly, changes in current direction are interpreted based on the orientation of the anomaly vectors, whereas the anomaly magnitude is used to assess the intensity of surface current variability.

Results and Discussion

To describe the dynamics of surface currents around Selayar Island, the results are organized based on analyses of the long-term mean (climatological mean), monthly variability, and differences among the ENSO phases. The long-term mean pattern of surface currents in the study area is obtained by averaging the data over the period 1993–2020 and is used to provide a general depiction of surface current conditions (Figure 1).

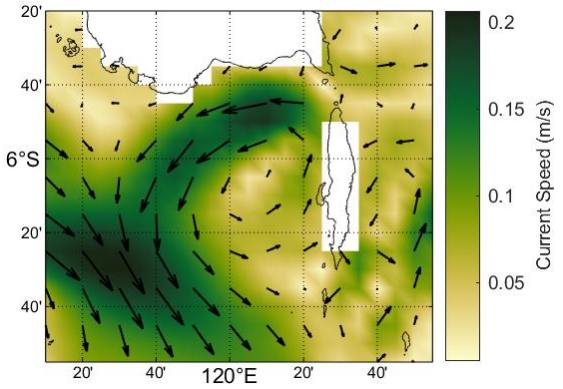

Figure 1. Long-term climatological mean (1993–2020) of sea surface currents around Selayar Island. Shading indicates the mean current speed (magnitude), while arrows represent the direction of the mean current vectors.

The long-term mean reveals a well-defined current corridor in the northwestern sector of Selayar Island that converges toward the main current pathway, representing a branch of the ITF extending toward the southwestern part of the domain, along with relatively weaker currents in the vicinity of the island. Within the main corridor, the flow direction is relatively uniform, whereas greater directional variability around Selayar Island reflects the influence of local topography on surface circulation. This spatial variability is consistent with the characteristics of the Selayar Slope region, which is shaped by shelf–slope topography and regional water mass interactions (Prihatiningsih et al., 2021).

Figure 2 presents the monthly climatology of surface currents, calculated as the mean for each month over the period 1993–2020. Compared to the 27-year long-term mean (Figure 1), the monthly climatology indicates that surface currents exhibit a pronounced seasonal cycle in both intensity and direction. Quantitatively, the domain-averaged monthly current magnitude ranges from 0.085 to 0.305 ms^{-1}. The highest domain-mean current speeds occur in January (~0.305 ms^{-1}), followed by February (~0.281 ms^{-1}) and December (~0.257 ms^{-1}). In contrast, the lowest domain-mean current speeds are observed in April (~0.085 ms^{-1}) and remain relatively

weak again in October (~0.093 ms^{-1}), coinciding with the seasonal transition periods. At the spatial scale, the maximum current magnitude within the domain reaches approximately 0.64–0.66 ms^{-1} during June–August as well as in January, indicating the presence of intensified current cores during specific months.

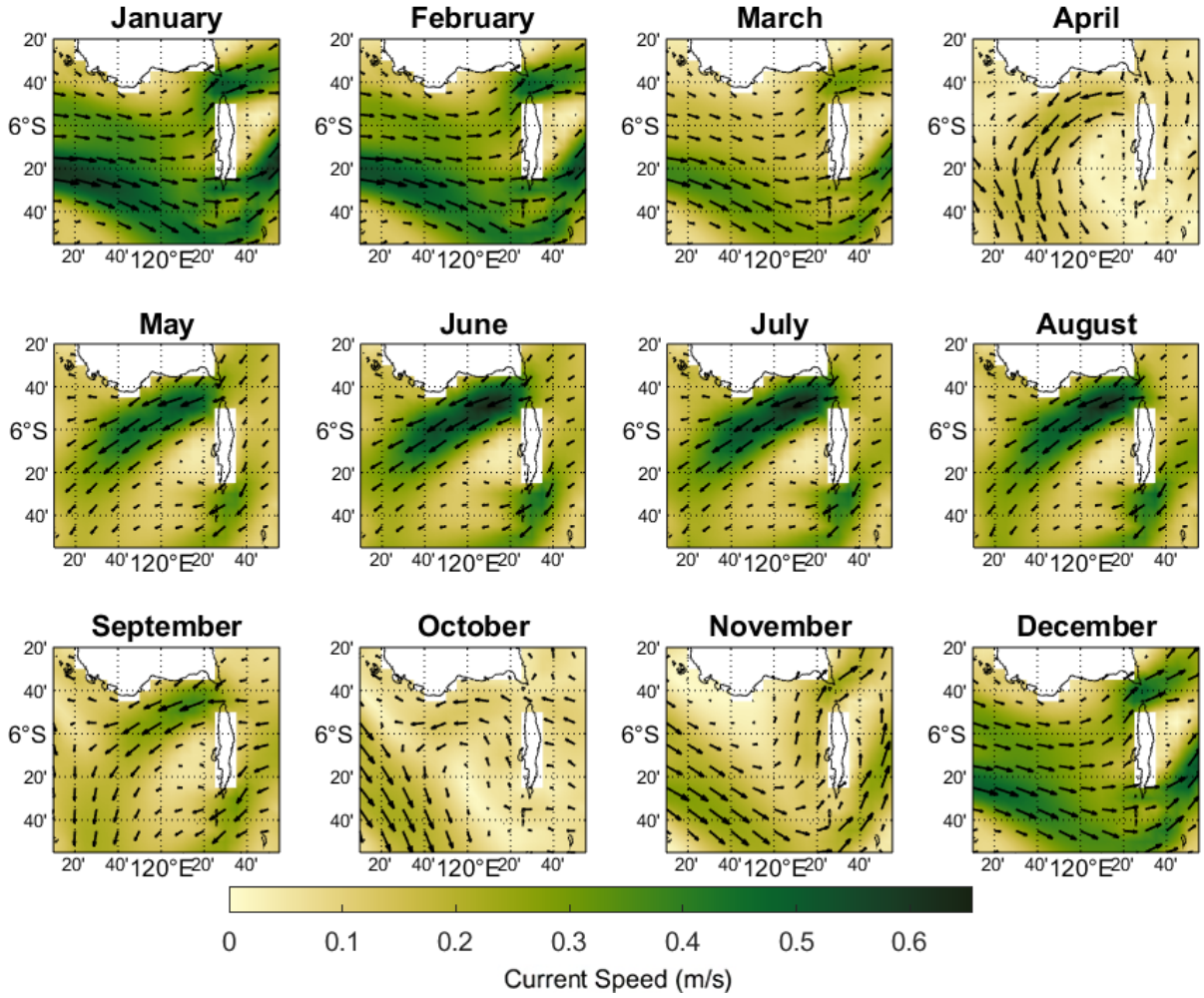

Figure 2. Monthly climatology of sea surface currents around Selayar Island based on the 27-year mean (1993–2020). Each panel shows the current speed magnitude (shading) and the direction of current vectors (arrows) for each month.

Seasonal changes in current direction are also clearly evident. Domain-averaged results show that during January–March and November–December, the mean zonal component tends to be eastward (positive *u*), whereas during May–September the mean zonal component is predominantly westward (negative *u*), accompanied by a generally southward mean meridional component (negative *v*). April and October are characterized by weaker current conditions and directional tendencies that differ from those observed during the peak monsoon months. This seasonal pattern is consistent with previous findings showing that surface currents around the Selayar Islands vary in response to the monsoonal cycle and transitional seasons (Bayhaqi et al., 2017), and it further reflects the strong monsoonal control and inter-basin connectivity that characterize circulation within the Indonesian Archipelago (Yoneyama & Zhang, 2020; Xue et al., 2020; Apriansyah et al., 2024).

Figure 3 presents the composite mean surface currents for the three ENSO phases based on the Niño-3.4 index: Neutral (N = 156 months), El Niño (N = 76 months), and La Niña (N = 104 months). The Niño-3.4

time series for the period 1993–2020 includes strong ENSO events, with peak positive anomalies reaching +2.72 °C in November 2015 and minimum anomalies reaching −1.77 °C in January 2000 (NOAA, 2026). Accordingly, the resulting composites represent an aggregation of weak to strong events within each ENSO phase.

Overall, all three ENSO phases preserve the primary spatial structure of surface currents around Selayar Island, but exhibit differences in mean intensity and vector configuration across several sectors of the domain. As shown in Figure 3, Neutral conditions are characterized by a relatively strong current flowing from the Selayar Strait toward the southwest and merging with the main current corridor. This feature is not observed during El Niño and La Niña phases, during which currents west of Selayar Island undergo deflection and form vortex-like circulation patterns, indicating the presence of localized circulation arising from current–topography interactions. In addition, during Neutral conditions, currents within the main corridor in the southwestern sector of the domain tend to be oriented predominantly in the north–south direction. In contrast, during El Niño and La Niña phases, the orientation of currents in the main corridor is more similar to the long-term climatological pattern, flowing from the northwest toward the southeast. Nevertheless, during La Niña conditions, currents within this corridor appear slightly stronger than those observed during El Niño.

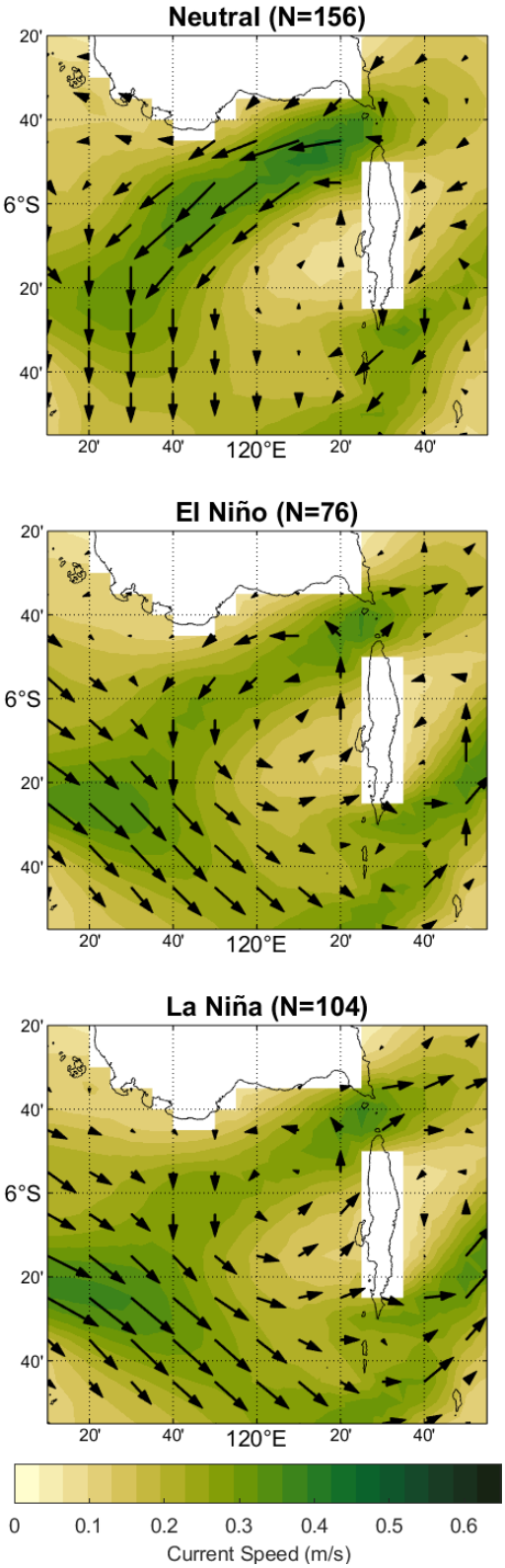

Figure 3. Composite mean sea surface currents for the three ENSO phases: Neutral, El Niño, and La Niña. Shading indicates the composite current speed magnitude, while arrows represent the direction of the composite current vectors. The composites are calculated by averaging the current components over the months corresponding to each ENSO phase.

To assess the extent to which surface current patterns under different ENSO phases deviate from the long-term mean state, the analysis is further focused on composite surface current anomalies. The composite anomaly results are shown in Figure 4. The direction of anomaly currents crossing the Selayar Strait exhibits clear differences among ENSO phases. Under Neutral conditions, current anomalies display a northeast-to-southwest flow crossing the Selayar Strait and extending into the southern part of Selayar Island. In contrast, during El Niño and La Niña phases, anomaly currents show opposite directions when crossing the Selayar Strait and the waters south of the island. In addition, the intensity of current anomalies during El Niño conditions appears weaker than that observed during La Niña conditions.

The composite anomaly patterns further reveal clear quantitative differences between the two phases. Domain averaged anomaly magnitudes are estimated to range from approximately 0.03–0.05 ms^{-1} during El Niño and increase to about 0.07–0.09 ms^{-1} during La Niña. The maximum anomaly magnitudes further highlight this contrast. During La Niña, peak anomaly values reach approximately 0.10–0.12 ms^{-1}, whereas during El Niño the maximum anomalies are generally limited to around 0.04–0.08 ms^{-1}. This indicates that surface current anomalies during La Niña are stronger by approximately 0.03–0.06 ms^{-1} compared to those during El Niño. Spatially, regions with relatively high anomaly magnitudes (>0.08 ms^{-1}) are more extensive during La Niña, while anomalies during El Niño tend to be weaker.

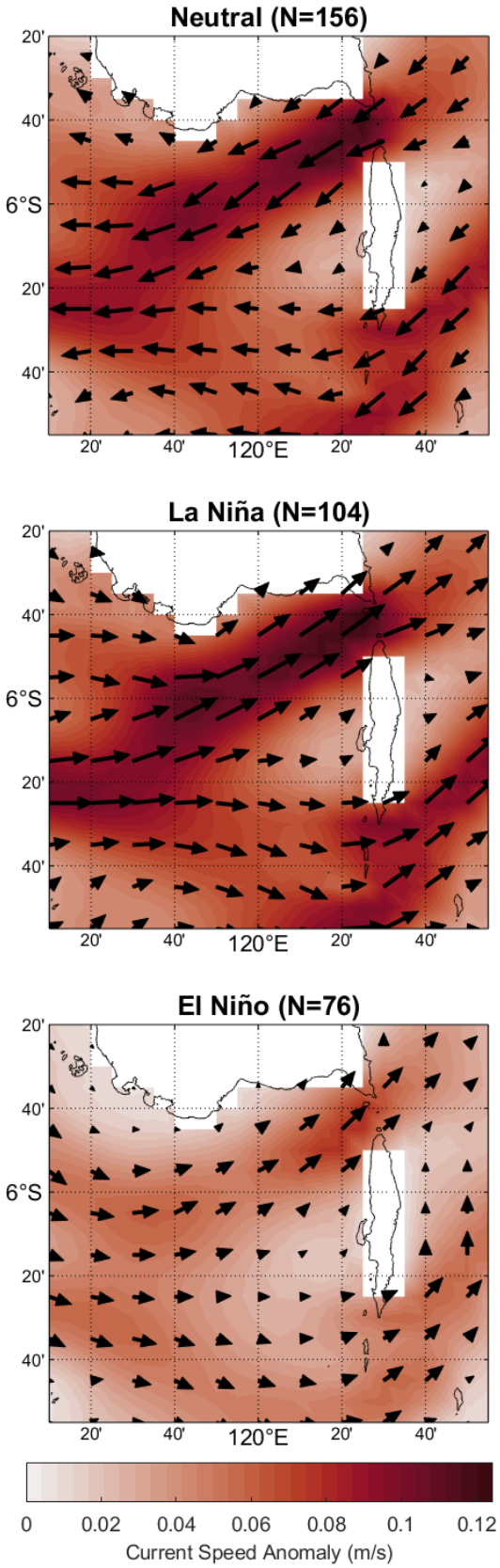

Figure 4. Same as Figure 3, but for composite sea surface current anomalies.

These results indicate that ENSO exerts a measurable influence on surface current

variability in the study region, with La Niña conditions enhancing current anomalies more effectively than El Niño. This asymmetry is consistent with previous studies indicating that La Niña is associated with strengthened large-scale circulation and increased ITF transport, which can amplify regional current variability (Feng et al., 2018; Gordon et al., 2019; Santoso et al., 2022).

In addition to these interannual differences, the results are further examined in the context of seasonal variability. The dominance of seasonal variability in the monthly climatological results confirms that monsoonal circulation is the primary driver of surface currents around Selayar Island. Changes in monsoon phases and transitional periods modulate both current intensity and direction, consistent with the characteristics of the Indonesian Archipelago, which is embedded within the coupled ocean and atmosphere system of the Maritime Continent (Yoneyama & Zhang, 2020; Xue et al., 2020).

Furthermore, the spatial heterogeneity evident in both the long-term climatological mean and the monthly climatology reflects the influence of local topography, particularly the Selayar Slope and island geometry, in modifying surface flow structures (Bayhaqi et al., 2017; Prihatiningsih et al., 2021). The inter-phase differences identified in the current composites and anomaly patterns indicate that ENSO acts as an interannual modulation of surface current dynamics in the study region. Nevertheless, the influence of ENSO on surface currents around Selayar Island appears to be weaker than that of seasonal variability, confirming that monsoonal forcing remains the dominant control on surface current dynamics in the region.

Several limitations should be considered when interpreting the results of this study. First, ENSO phase–based composites may be subject to seasonal sampling bias because the distribution of El Niño, La Niña, and Neutral months is not uniform throughout the year, while surface currents in the study region are strongly influenced by monsoonal variability. Second, the surface current data are derived from a reanalysis product; although this product assimilates a wide range of observations, the results remain dependent on the underlying model configuration and data assimilation schemes. Third, defining surface currents as an average over the upper layers (approximately 0.49–5 m) may limit the representation of very shallow processes or those strongly influenced by instantaneous wind forcing.

Conclusion

This study demonstrates that surface currents around Selayar Island exhibit a spatially heterogeneous structure and are primarily controlled by seasonal variability. Both the long-term climatological mean and the monthly climatology confirm the dominant role of monsoonal circulation in modulating the intensity and direction of surface currents. Seasonal variability produces larger changes in current direction and strength than interannual variability, indicating that monsoonal dynamics constitute the primary control on surface currents in the study region.

Interannual variability associated with ENSO is also evident, particularly in the magnitude of surface current anomalies. Quantitatively, surface current anomalies during El Niño range from approximately 0.03–0.05 ms^{-1} while anomalies during La Niña increase to about 0.07–0.09 ms^{-1}, with peak values reaching ~0.10–0.12 ms^{-1}. This indicates that anomalies during La Niña are stronger by approximately 0.03–0.06 ms^{-1} compared to those during El Niño. Notably, differences in the direction of surface current anomalies are more pronounced under Neutral conditions, where anomaly directions differ markedly from those

observed during both El Niño and La Niña phases.

Overall, these results indicate that ENSO acts as an interannual modulation of surface current intensity, superimposed on dominant seasonal forcing and local topographic influences. Despite this modulation, the influence of ENSO remains secondary to the strong control exerted by monsoonal circulation.

Acknowledgements

The authors would like to express their sincere gratitude to the editor and the anonymous reviewers for their constructive comments and suggestions that helped improve the quality and clarity of this manuscript. The authors also thank Fakhira Raisha for her support during the preparation of this study. No specific funding was received for this research.

Author Contribution

Andika**:** Conceptualization, Methodology, Data curation, Formal analysis, Visualization, Writing original draft, Writing-review & editing. Gladiva Warouw: Data collection, Reference collection, English language editing.

Conflict of Interest

The author declares no conflict of interest.

References

Apriansyah, A., Atmadipoera, A. S., Natih, N. M. N., Nugroho, D., Zuraida, R., Hartanto, M. T., & Syahdan, M. (2024). Water mass exchange in triangle seas of the Java-Makassar-Flores (JMF): A modeling study. *Continental Shelf Research*, 275, 105225. https://doi.org/10.1016/j.csr.2024.105225

Bayhaqi, A., Iskandar, M. R., & Surinati, D. (2017). Surface current pattern and physics condition of waters around Selayar Island in the first transitional and southeast monsoons. *Journal Oseanologi dan Limnologi di Indonesia*, 2(1), 83–95. https://doi.org/10.14203/oldi.2017.v2i1.71

Bhattacharya, B., Hossain, S. K. A., & Ghosh, M. (2026). Leveraging cloud-based SAR remote sensing and GNOME numerical simulation for modeling oil spill trajectory in the Black Sea. *Marine Pollution Bulletin*, 224, 119166. https://doi.org/10.1016/j.marpolbul.2025.119166

Boschat, G., Simmonds, I., Purich, A., Cowan, T., & Pezza, A. B. (2016). On the use of composite analyses to form physical hypotheses: An example from heat wave–SST associations. *Scientific Reports*, 6(1), 29599. https://doi.org/10.1038/srep29599

Bosi, S., Broström, G., & Roquet, F. (2021). The role of Stokes drift in the dispersal of North Atlantic surface marine debris. *Frontiers in Marine Science*, 8, 697430. https://doi.org/10.3389/fmars.2021.697430

Chassignet, E. P., Xu, X., & Zavala-Romero, O. (2021). Tracking marine litter with a global ocean model: where does it go? Where does it come from?. *Frontiers in Marine Science*, 8, 667591. https://doi.org/10.3389/fmars.2021.667591

Córdova, P., & Flores, R. P. (2022). Hydrodynamic and Particle Drift Modeling as a Support System for Maritime Search and Rescue (SAR) Emergencies: Application to the C-212 Aircraft Accident on 2 September, 2011, in the Juan Fernández Archipelago, Chile. *Journal of Marine Science and Engineering*, 10(11), 1649. https://doi.org/10.3390/jmse10111649

Devis-Morales, A., Rodríguez-Rubio, E., & Montoya-Sánchez, R. A. (2021). Modelling the transport of sediment discharged by Colombian rivers to the southern Caribbean Sea. *Ocean Dynamics*, 71(2), 251–277. https://doi.org/10.1007/s10236-020-01431-y

Elzahaby, Y., Schaeffer, A., Roughan, M., & Delaux, S. (2021). Oceanic circulation drives the deepest and longest marine heatwaves in the East Australian Current system. *Geophysical Research Letters*, 48(17), e2021GL094785. https://doi.org/10.1029/2021GL094785

Emery, W. J., & Thomson, R. E. (2001). *Data analysis methods in physical oceanography* (2nd ed.). Elsevier.

Feng, M., Zhang, N., Liu, Q., & Wijffels, S. (2018). The Indonesian throughflow, its variability and centennial change. *Geoscience Letters*, 5(1), 3. https://doi.org/10.1186/s40562-018-0102-2

Fu, Y., Wang, Z., Zhao, M., Song, X., Jia, Y., & Song, Z. (2024). Factors influencing the variation of the Sepik-Ramu River system's sediment plume off the north coast of New Guinea. *Estuarine, Coastal and Shelf Science*, 303, 108782. https://doi.org/10.1016/j.ecss.2024.108782

Gao, Y., Kamenkovich, I., Perlin, N., & Kirtman, B. (2022). Oceanic advection controls mesoscale mixed layer heat budget and air–sea heat exchange in the southern ocean. *Journal of Physical Oceanography*, 52(4), 537–555. https://doi.org/10.1175/JPO-D-21-0063.1

Gordon, A. L., Napitu, A., Huber, B. A., Gruenburg, L. K., Pujiana, K., Agustiadi, T., Kuswardani, A., Mbay, N., & Setiawan, A. (2019). Makassar Strait throughflow seasonal and interannual variability: An overview. *Journal of Geophysical Research: Oceans*, 124(6), 3724–3736. https://doi.org/10.1029/2018JC014502

Halide, H., Wulandari, P., & Andika, A. (2024). New metrics for distinguishing the skill of long-range ENSO forecasting models. *AIP Conference Proceedings*, 2774(1), 050005. https://doi.org/10.1063/5.0164472

Hartmann, D. L. (2016). *Global physical climatology* (2nd ed.). Elsevier.

Hu, Q., Chen, X., Huang, W., & Zhou, F. (2021). Phytoplankton bloom triggered by eddy-wind interaction in the upwelling region east of Hainan Island. *Journal of Marine Systems*, 214, 103470. https://doi.org/10.1016/j.jmarsys.2020.103470

Isern-Fontanet, J., Ballabrera-Poy, J., Turiel, A., & García-Ladona, E. (2017). Remote sensing of ocean surface currents: A review of what is being observed and what is being assimilated. *Nonlinear Processes in Geophysics*, 24(4), 613–643. https://doi.org/10.5194/npg-24-613-2017

Jean-Michel, L., Eric, G., Romain, B-B., Gilles, G., Angélique, M., Marie, D., Clément, B., Mathieu, H., Olivier, L. G., Charly, R., Tony, C., Charles-Emmanuel, T., Florent, G., Giovanni, R., Mounir, B., Yann, D., & Pierre-Yves, L. T. (2021). The Copernicus global 1/12 oceanic and sea ice GLORYS12 reanalysis. *Frontiers in Earth Science*, 9, 698876. https://doi.org/10.3389/feart.2021.698876

Keramea, P., Spanoudaki, K., Zodiatis, G., Gikas, G., & Sylaios, G. (2021). Oil spill modeling: A critical review on current trends, perspectives, and challenges. *Journal of Marine Science and Engineering*, 9(2), 181. https://doi.org/10.3390/jmse9020181

L'Heureux, M. L., Tippett, M. K., Wheeler,

M. C., Nguyen, H., Narsey, S., Johnson, N., Hu, Z., Watkins, A. B., Lucas, C., Ganter, C., Becker, E., Wang, W., & Di Liberto, T. (2024). A relative sea surface temperature index for classifying ENSO events in a changing climate. *Journal of Climate*, 37(4), 1197–1211. https://doi.org/10.1175/JCLI-D-23-0406.1

Laurindo, L. C., Siqueira, L., Small, R. J., Thompson, L., & Kirtman, B. P. (2024). Quantifying the contribution of ocean advection and surface flux to the upper-ocean salinity variability resolved by climate model simulations. *Geophysical Research Letters*, 51(3), e2023GL106354. https://doi.org/10.1029/2023GL106354

Lefebvre, C., Le Bihanic, F., Jalón-Rojas, I., Dusacre, E., Chassaigne--Viscaïno, L., Bichon, J., Clérandeau, C., Morin, B., Lecomte, S., & Cachot, J. (2023). Spatial distribution of anthropogenic particles and microplastics in a meso-tidal lagoon (Arcachon Bay, France): A multi-compartment approach. *Science of The Total Environment*, 898, 165460. https://doi.org/10.1016/j.scitotenv.2023.165460

Li, L., & Dolman, A. J. (2023). On the reliability of composite analysis: an example of wet summers in North China. *Atmospheric Research*, 292, 106881. https://doi.org/10.1016/j.atmosres.2023.106881

Li, S., Zhang, Z., Zhou, M., Wang, C., Wu, H., & Zhong, Y. (2022). The role of fronts in horizontal transports of the Changjiang River plume in summer and the implications for phytoplankton blooms. *Journal of Geophysical Research: Oceans*, 127(8), e2022JC018541. https://doi.org/10.1029/2022JC018541

Lu, Z., Gan, J., Dai, M., Zhao, X., & Hui, C. R. (2020). Nutrient transport and dynamics in the South China Sea: A modeling study. *Progress in Oceanography*, 183, 102308. https://doi.org/10.1016/j.pocean.2020.102308

Mannarini, G., Salinas, M. L., Carelli, L., Petacco, N., & Orović, J. (2024). VISIR-2: Ship weather routing in Python. *Geoscientific Model Development*, 17(10), 4355–4382. https://doi.org/10.5194/gmd-17-4355-2024

Manral, D., Iovino, D., Jaillon, O., Masina, S., Sarmento, H., Iudicone, D., Amaral-Zettler, L., & van Sebille, E. (2023). Computing marine plankton connectivity under thermal constraints. *Frontiers in Marine Science*, 10, 1066050. https://doi.org/10.3389/fmars.2023.1066050

Mappong, S. (2018, 3 Juli). *KM Lestari Maju tujuan Selayar tenggelam*. ANTARA News. https://www.antaranews.com/berita/723622/km-lestari-maju-tujuan-selayar-tenggelam?

Mateus, M., Canelas, R., Pinto, L., & Vaz, N. (2020). When tragedy strikes: potential contributions from ocean observation to search and rescue operations after drowning accidents. *Frontiers in Marine Science*, 7, 00055. https://doi.org/10.3389/fmars.2020.00055

Mercator Ocean International. (2026). Global Ocean Physics Reanalysis [Data set]. Copernicus Marine Service (CMEMS). https://doi.org/10.48670/moi-00021

Nie, X., Liu, H., Xu, T., & Wei, Z. (2023). Influence of the El Niño-Southern Oscillation on upper-ocean salinity changes in the southeast Indian ocean. *Frontiers in Marine Science*, 10, 1181278. https://doi.org/10.3389/fmars.2023.1181278

NOAA (2026). *Niño 3.4 monthly time-*

series dataset [Data set]. NOAA Physical Sciences Laboratory. https://psl.noaa.gov/data/timeseries/month/DS/Nino34_CPC/

Prihatiningsih, I., Jaya, I., Atmadipoera, A. S., & Zuraida, R. (2021). Stratification and characteristic of water masses in Selayar Slope-Southern Makassar Strait. *Omni-Akuatika*, 17(1), 27–36. http://dx.doi.org/10.20884/1.oa.2021.17.1.620

Purba, N. P., Faizal, I., Christie, D., Pratama, M. B., Valino, D. A., Martasuganda, M. K., Herawati, T., Wulandari, A., Utami, S. T., Aryanto, N. C. D., Ilmi, M. H., Alfarez R. R., & Pasaribu, B. (2024). Mapping the sources and strands of marine debris via particle modelling and In-situ sampling approaches in archipelagic countries. *Scientific Reports*, 14(1), 25804. https://doi.org/10.1038/s41598-024-73373-0

Ralston, D. K., Geyer, W. R., Wackerman, C. C., Dzwonkowski, B., Honegger, D. A., & Haller, M. C. (2024). Interacting influences of diurnal tides, winds, and river discharge on a large coastal plume. *Journal of Geophysical Research: Oceans*, 129(9), e2024JC021288. https://doi.org/10.1029/2024JC021288

Röhrs, J., Sutherland, G., Jeans, G., Bedington, M., Sperrevik, A. K., Dagestad, K. F., Gusdal Y., Mauritzen, C., Dale A., & LaCasce, J. H. (2023). Surface currents in operational oceanography: Key applications, mechanisms, and methods. *Journal of Operational Oceanography*, 16(1), 60–88. https://doi.org/10.1080/1755876X.2021.1903221

Said, N. H. (2024, 11 Agustus). *Kapal muat 5.000 sak semen tenggelam di Selayar, 8 ABK-penumpang selamat*. https://www.detik.com/sulsel/berita/d-7483896/kapal-muat-5-000-sak-semen-tenggelam-di-selayar-8-abk-penumpang-selamat?

Santoso, A., England, M. H., Kajtar, J. B., & Cai, W. (2022). Indonesian Throughflow variability and linkage to ENSO and IOD in an ensemble of CMIP5 models. *Journal of Climate*, 35(10), 3161–3178. https://doi.org/10.1175/JCLI-D-21-0485.1

Stewart, R. H. (2008). *Introduction to physical oceanography*. Texas A&M University.

Tamtare, T., Dumont, D., & Chavanne, C. (2022). The Stokes drift in ocean surface drift prediction. *Journal of Operational Oceanography*, 15(3), 156–168. https://doi.org/10.1080/1755876X.2021.1872229

Trinanes, J. A., Olascoaga, M. J., Goni, G. J., Maximenko, N. A., Griffin, D. A., & Hafner, J. (2016). Analysis of flight MH370 potential debris trajectories using ocean observations and numerical model results. *Journal of Operational Oceanography*, 9(2), 126–138. https://doi.org/10.1080/1755876X.2016.1248149

Vijith, V., Vinayachandran, P. N., Webber, B. G., Matthews, A. J., George, J. V., Kannaujia, V. K., Lotliker, A. A., & Amol, P. (2020). Closing the sea surface mixed layer temperature budget from in situ observations alone: Operation Advection during BoBBLE. *Scientific reports*, 10(1), 7062. https://doi.org/10.1038/s41598-020-63320-0

Wang, J., Qin, H., Wang, D., Li, Z., Li, B., Su, H., Liu, C., Qin, L., Tu, H., & Mu, L. (2025). Research on drift trajectories of typical marine search and rescue objects based on wind-wave-current coupled experiments. *Applied Ocean Research*, 165, 104827. https://doi.org/10.1016/j.apor.2025.104827

Wardiyah, N. S. (2024, 8 Januari). *Bupati Selayar salurkan santunan ke ahli waris korban kapal tenggelam*. ANTARA News. https://www.antaranews.com/berita/3905547/bupati-selayar-salurkan-santunan-ke-ahli-waris-korban-kapal-tenggelam?

Wei, L. (2024). Summary of Commonly Used ENSO Indices. *Highlights in Science, Engineering and Technology*, 88, 687-694. https://doi.org/10.54097/vndv3190

Wilks, D. S. (2011). *Statistical methods in the atmospheric sciences* (3rd ed.). Academic Press.

Xue, P., Malanotte-Rizzoli, P., Wei, J., & Eltahir, E. A. B. (2020). Coupled ocean-atmosphere modeling over the Maritime Continent: A review. *Journal of Geophysical Research: Oceans*, 125(6), e2019JC014978. https://doi.org/10.1029/2019JC014978

Yoneyama, K., & Zhang, C. (2020). Years of the maritime continent. *Geophysical Research Letters*, 47(12), e2020GL087182. https://doi.org/10.1029/2020GL087182

Zhu, K., Mu, L., Yu, R., Xia, X., & Tu, H. (2023). Probabilistic modelling of surface drift prediction in marine disasters based on the NN–GA and ARMA model. *Ocean Engineering*, 281, 114804. https://doi.org/10.1016/j.oceaneng.2023.114804

Zhu, Q., & Wang, C. (2024). Contributions of Indo-Pacific forcings to interannual variability of the Indonesian Throughflow in the upper and lower layers. *Journal of Geophysical Research: Oceans*, 129(1), e2023JC020306. https://doi.org/10.1029/2023JC020306